8.3

MODEL SIMULATIONS OF EXTREME OROGRAPHIC PRECIPITATION IN THE SIERRA NEVADA DURING THE NEW YEAR'S HOLIDAY FLOOD OF 2005-06

Phillip J. Marzette*, Michael L. Kaplan and Chris Adaniya
Division of Atmospheric Sciences, Desert Research Institute, Reno, Nevada

James Wallman and Rhett Milne
National Weather Service, Reno, Nevada

ABSTRACT

Forecasting precipitation in mountainous regions is a very demanding and arduous task. Some examples of devastating flooding events in mountainous areas include the Big Thompson Flood of 1976 in the Rocky Mountains (Maddox 1978) and the Piedmont flood event of 1994 in the Alps (Buzzi et al. 1998). The flooding events in the Sierra Nevada during 1997 and 2005 had a major impact on the Truckee River Valley including the Reno metropolitan area, however not much has been documented with either case. Both flooding events in Reno involved the passage of upper-level cold fronts that enabled ageostrophic and diabatic adjustments to create processes that led to flooding rains. It is the juxtaposition of the cold front aloft, tropical air stream from the South Pacific and complex terrain that led to the extreme lee side liquid precipitation accumulation to a significant elevation. This paper focuses on the 2005 event. A verification of the simulation of the 2005 case study employing the Operational Multiscale Environment model with Grid Adaptivity (OMEGA) (e.g., Bacon et al. 2000) was performed. What makes OMEGA a novel approach for modeling research and forecasting is that it employs an unstructured grid that can be used to adapt to certain features like clouds and terrain, therefore enhancing the local resolution of key orographic forcing features. The OMEGA adaptive grid simulations were performed with static grid adaptivity to 1 km resolution over the Sierra Nevada. These simulations were then validated against asynoptic and synoptic observations including Doppler and surface rainfall observations. The goal for this research is to 1) explore whether or not an unstructured, static, adaptive grid will produce accurate simulations of an extreme lee side rainfall event and 2) to aid forecasters in understanding the precursor physical and dynamical processes which cause such an event.

1. INTRODUCTION

The eastern Sierra Nevada and Truckee Meadows has experienced several heavy precipitation events through the years. Some examples include flooding rainfall events on 14-19 February 1986 and 1-3 January 1997, as well as two heavy snowfall events in 30-31 December 2004 and 7-8 January 2005. These dates indicate that a heavy precipitation event can happen at least once every few years. This paper will focus attention on the flooding rainfall event of 30 December 2005-1 January 2006. This event produced copious amounts of rainfall that enabled the Truckee River to exceed flood stage. The excess water flooded the Reno-Sparks metropolitan area, causing millions of dollars in damage.

The precipitation totals for this event were 4.5 inches for South Lake Tahoe, CA, 8.46 inches for Blue Canyon/Emigrant Gap, CA and 1.7 inches for Reno, NV. The rainfall amount in Reno, while meager in comparison to some of the sites that are on the windward side and the crest of the Sierra Nevada, represented an extreme local precipitation event. This would suggest that organizing dynamic features allowed heavy rainfall amounts well downstream of the lee side of the Sierra Nevada. The result of these dynamic features has been referred to by various authors (e.g., Browning 1975; Sinclair 1994, 1997; Colle 2004) as precipitation that has “spilled over” on to the lee side of mountain ranges. Some of the heavier bursts of precipitation on the lee side of the Carson Range during 0000-0600 and 1500-2100 UTC 31 December 2005 (Figs. 1a and 1b) show that spillover rainfall was present.

*Corresponding author address: Phillip Marzette, Division of Atmospheric Sciences, Desert Research Institute, Reno, NV 89512. E-Mail: marzette@dri.edu

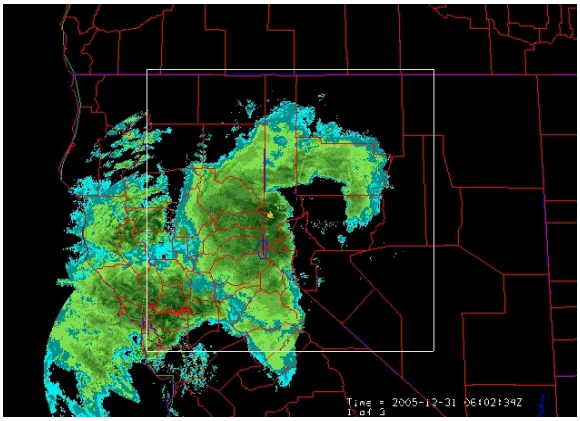

(a)

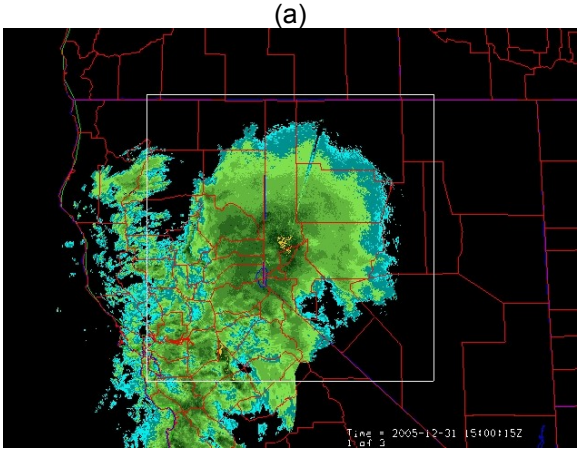

(b)

Figure 1: Composite NEXRAD Doppler reflectivity images for (a) 0600 and (b) 1500 UTC 31 December 2005. Radar sites are from Beale Air Force Base, CA; San Francisco, CA; Sacramento, CA and Reno, NV.

2. OBSERVATIONAL SUMMARY

In order for spillover precipitation to occur on the lee side, high wind velocities over the mountain crest, a low freezing level relative to the surface and unstable air are necessary (Colle 2004). The North American Regional Reanalysis (NARR) data will serve as the observed fields. During the first heavy precipitation event, i.e. 0000-0600 UTC, the polar jet streak at 250 hPa is slowly propagating to the southeast, changing Reno's orientation relative to the jet from the right exit region to the left exit region (Fig. 2a). This is more favorable for diffluent flow at upper-levels, mass flux divergence and upward environmental motion. When this 250 hPa jet streak's left exit region moves over Reno and the lee side of the Sierras on 0600 UTC 31 December, the low-level return branch flow is established, creating instability and upward motion in the moist environment that takes place in the exit region of a low to mid-level jet streak (Fig. 2b; Uccellini and Johnson 1979; Kaplan et al. 1998). Additionally, this lower level jet streak is simultaneously transporting warm Pacific moist air over the Sierras under the upper-level jet exit region (Fig. 2c). Thus the vertical lee side structure includes a south-southwesterly low-level return branch, low to mid west-southwesterly moist tongue and mid-upper tropospheric left exit region cold pool. The leading edge of the cold pool is beginning to strengthen aloft (Fig. 2d), so that lee side ascent and cold air advection overrun the low-level flow, where converging winds occur at the surface. Decreasing mean sea level pressure to 994 hPa (Fig. 2e) near the Oregon-California state line occurs under the exit region (Locatelli et al. 1997). This newly created meso low just east of the Sierra Crest will subsequently lead to convergence, upward vertical motion (Fig. 2f), and heavy rainfall on the lee side. A second heavy precipitation event occurs during 1500-2100 UTC that once again is due to a phasing of the jet streaks between mid and upper levels. However, with this second event the upper-level cold air advection is more dominant, thus decreasing the static stability simultaneously and deepening the existing meso low further. The moist air is advected to the lee side thus enabling this second heavy burst of precipitation (Figs. 3a-3f).

3. SIMULATION EXPERIMENTS

In order to solve the extraordinary problems associated with the forecasting of heavy precipitation events in complex terrain such as the Sierra Nevada, a suitable numerical weather prediction model was needed. The Operational Multiscale Environmental model with Grid Adaptivity (OMEGA) was the numerical weather prediction used here because the high-resolution triangular grid employed is beneficial for adapting to complex terrain, thus *efficiently* placing the resolution where it is needed in the most complex terrain (Bacon et al. 2000). Our numerical sensitivity study focused on the importance of initial data employed in the numerical model. The control experiment used the aviation (AVN) quasi-regular octant grid and the experimental run used the NCEP/NCAR reanalysis data (Kalnay et al. 1996). The main difference between the two data sets is the NCEP/NCAR data set has more layers with high resolution observations incorporated compared to the AVN data set. The hypothesis posed prior to the numerical simulations was that a data set with more layers and asynoptic

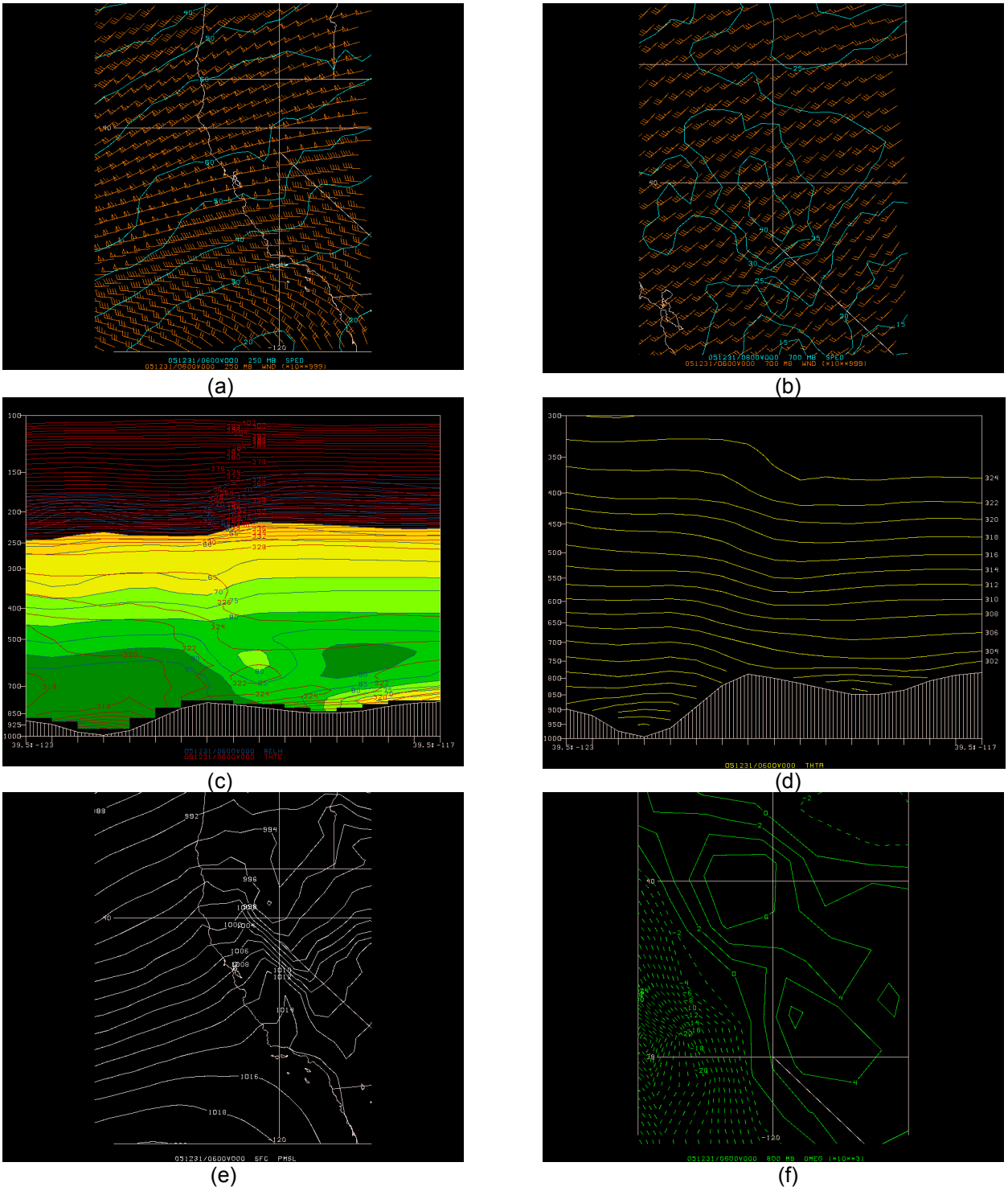

Figure 2: North American Regional Reanalysis (NARR) data of the (a) 250 hPa and (b) 700 hPa isotachs and wind barbs (m s^{-1}). Cross sections profiling the (c) moisture and instability and (d) potential temperature (θ) of the eastern Sierra Nevada and northwestern Nevada (39.5°N, 123°W – 39.5°N, 117°W; ref. Fig. 4c). In (c), yellow and green filled blue contours represent relative humidity (%) and the red lines are equivalent potential temperature (θ_e) at 2 K intervals. The θ contours in (d) are also in 2 K intervals. (e) Mean sea level pressure (MSLP; hPa) and (f) 800 hPa vertical motion (μb s^{-1}), where rising (sinking) motion is indicated by dashed (solid) lines. All times are for 0600 UTC 31 December 2005.

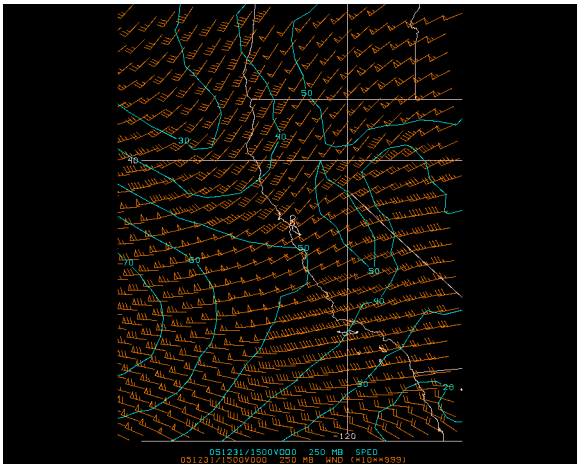

(a)

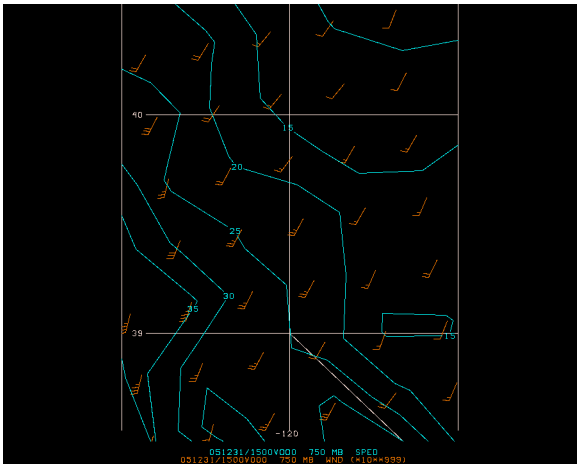

(b)

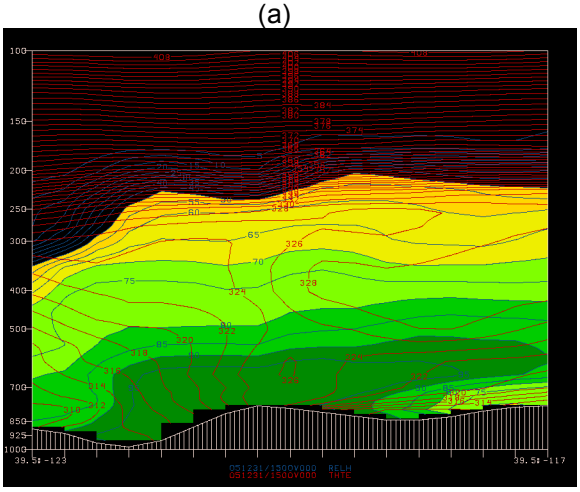

(c)

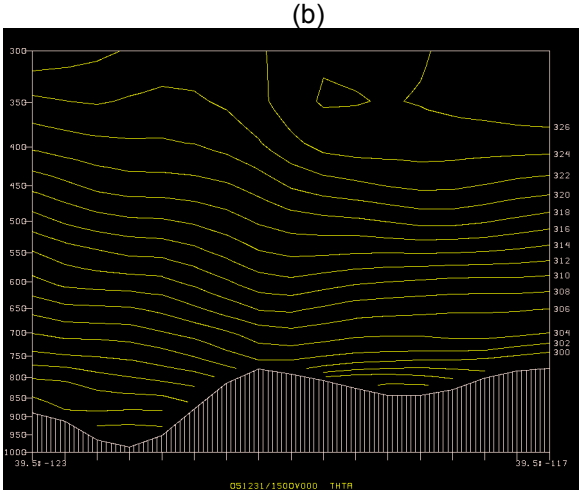

(d)

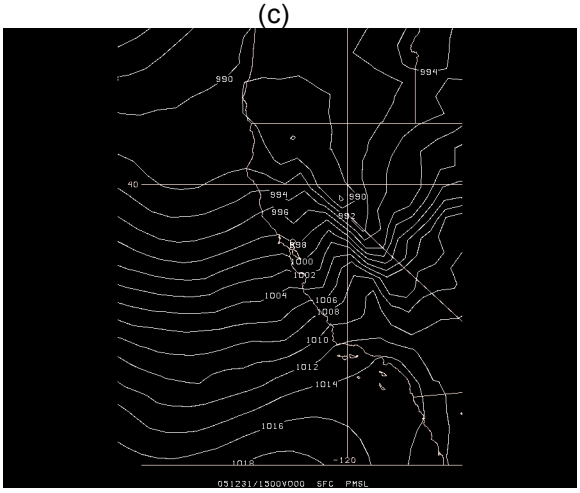

(e)

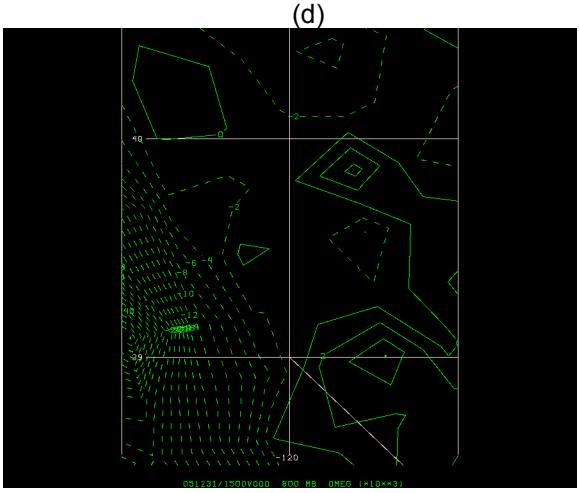

(f)

Figure 3: Figures 3a, 3c-3f are the same fields as Figures 2a, 2c-2f. Figure 3b is the 750 hPa isotachs and wind barbs. All times are for 1500 UTC 31 December 2005.

information would produce a more accurate and detailed simulation.

The physics employed for the two model simulations were identical and included the Kuo-Anthes (1977) convective parameterization scheme and a modified Lin et al. (1983) microphysical scheme. There were 34 unevenly spaced sigma vertical levels in these simulations and the horizontal resolution was 20 km for the coarse mesh, 5 km for the fine mesh and 1 km for the very fine mesh. Lateral boundary conditions were from observations for the coarse mesh. The 1 kilometer resolution covered the Reno-Lake Tahoe area (Figs. 4a and 4b). Both simulations used identical static grids, meaning the grid remained fixed and adapted to the terrain for this experiment. The model runs were initialized at 1200 UTC 30 December 2005 and simulated for 36 hours.

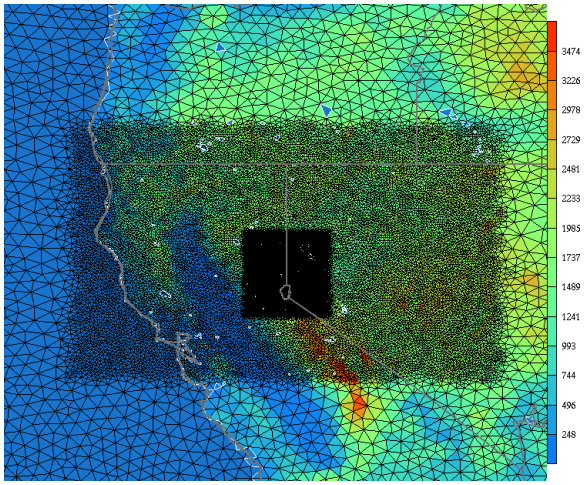

(a)

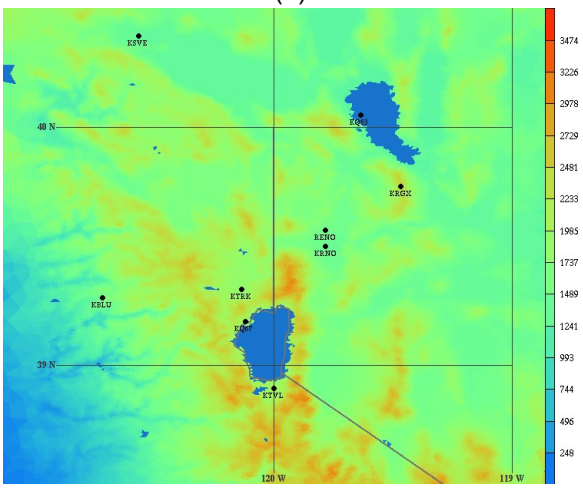

(b)

Figure 4: Image of the (a) grid mesh that is going to be used for the two OMEGA model simulations. The 1 km mesh is surrounded by the 5 km mesh, which is surrounded by the 20 km mesh. The 1 km terrain is highlighted in (b), where the Sierra Crest is to the west of Lake Tahoe and the Carson Range is to the east of Lake Tahoe. The terrain height (m) is the current field setting for (a) and (b).

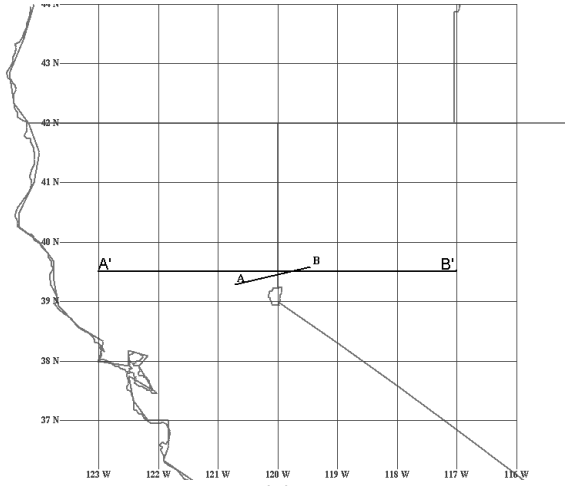

(c)

Figure 4 (cont.): Cross section plan views (c) for A' – B' (Figures 2c, 2d, 3c and 3d) and A – B (Figures 5g-5j, 6g-6j, and 7a-7d).

Figs. 5a and 5b show the 0600 UTC 31 December 2005 250 hPa jet for the AVN and NCEP/NCAR reanalysis respectively. The NCEP/NCAR jet indicates that there is stronger diffluent flow in the exit region over northern California and the Sierra Nevada compared to the AVN data. At 700 hPa, the lower-level jet streak is a little further to the southeast in the NCEP/NCAR reanalysis than the AVN (Figs. 5c and 5d). The mean sea level pressure (MSLP) in the AVN data is 999 hPa in the Reno area (Fig. 5e) while the NCEP/NCAR reanalysis data has a MSLP of 997 hPa in the same area (Fig. 5f), suggesting that the mass flux divergence aloft is stronger and the low-level return branch circulation is stronger, thus converging more mass near the heavy rainfall region in the NCEP/NCAR simulation than in the AVN simulation. The potential instability profile inferred from the equivalent potential temperature (θ_e) cross sections at 0600 UTC 31 December (Figs. 5g and 5h) show that the NCEP/NCAR reanalysis has less stable air on the lee of the Carson Range at mid-levels with θ_e hovering around 318 K between 3-5 km above the surface, while the AVN shows virtually little to no change of θ_e with increasing height in the 3-5 km layer. *Thus*

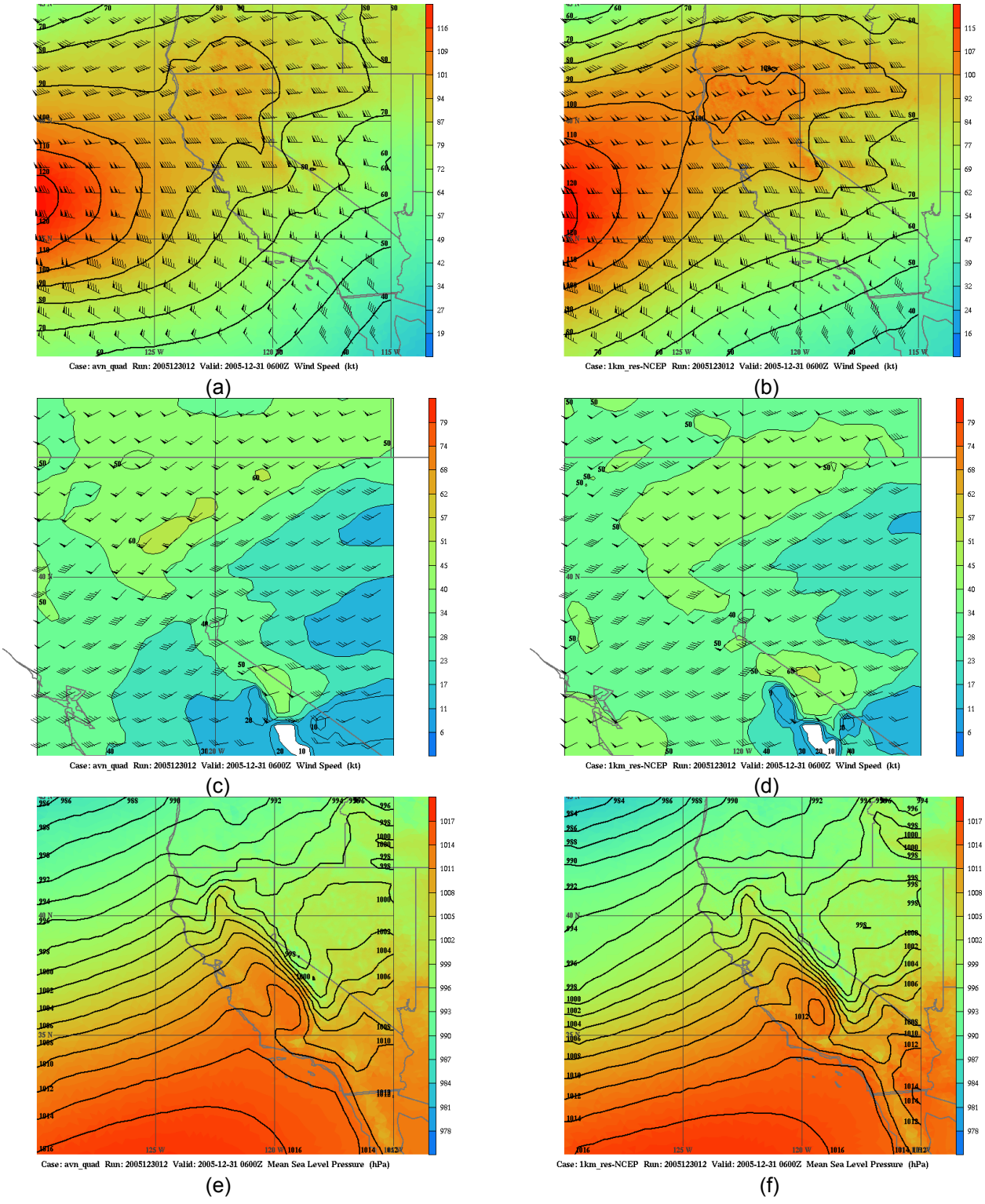

Figure 5: 250 hPa isotachs and wind barbs (knots; 1 m s^{-1} = 1.943 knots) of the (a) aviation (AVN) quasi-regular octant simulation and (b) NCEP/NCAR reanalysis simulation. 700 hPa isotachs and wind barbs of the (c) AVN and (d) NCEP/NCAR reanalysis simulation. MSLP for the (e) AVN and (f) NCEP/NCAR simulations. All times are for 0600 UTC 31 December 2005.

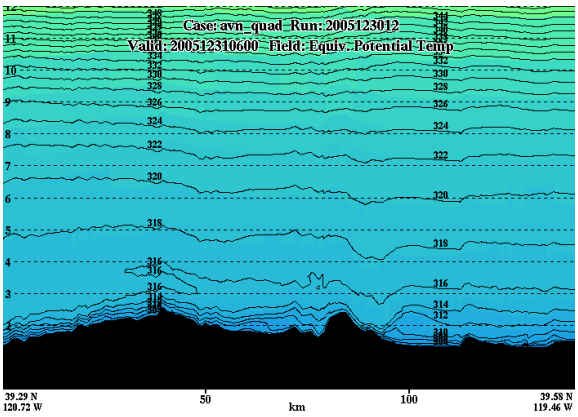

(g)

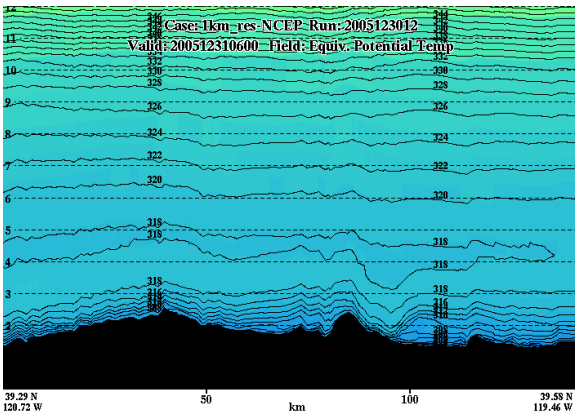

(h)

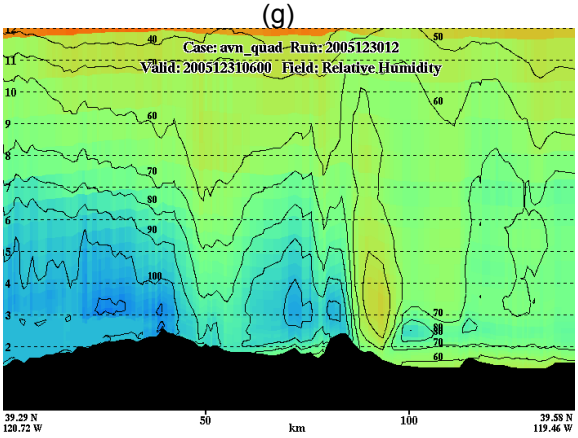

(i)

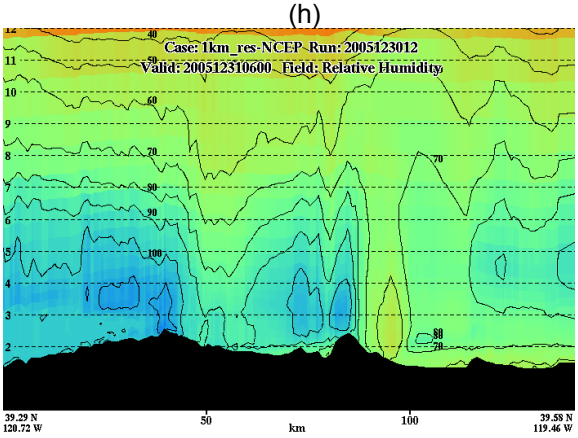

(j)

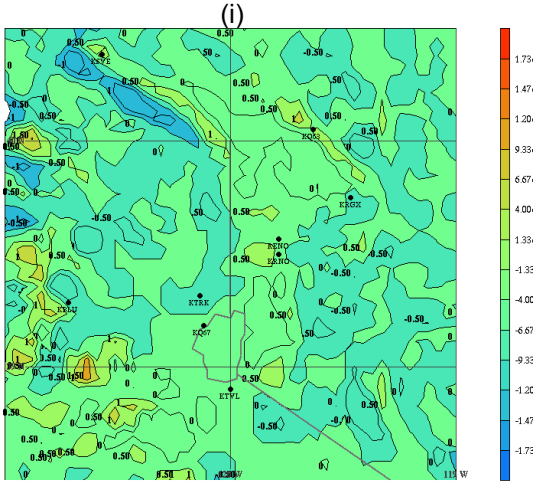

(k)

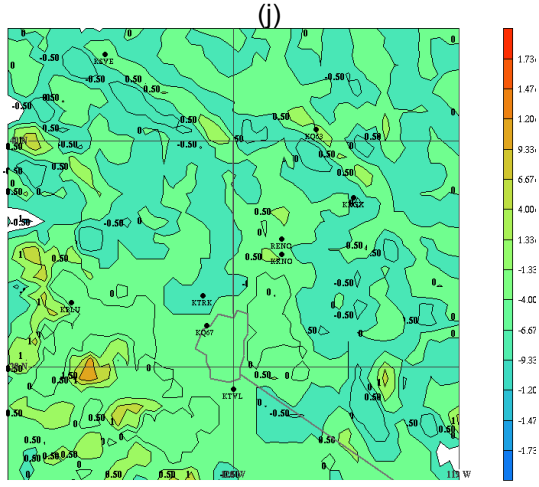

(l)

Figure 5 (cont.): Cross sections of (g and h) θ_e and (i and j) relative humidity for the AVN simulations (g and i) and the NCEP/NCAR simulations (h and j). The cross section covers from Blue Canyon, CA to south of Virginia Peak, NV (39.29°N, 120.72°W – 39.58°N, 119.46°W; ref. Fig. 4c). 800 hPa vertical velocity field (m s^{-1}; 1 cm s^{-1} ≈ 1 μb s^{-1}) for the (k) AVN and (l) NCEP/NCAR simulations. All times are for 0600 UTC 31 December 2005.

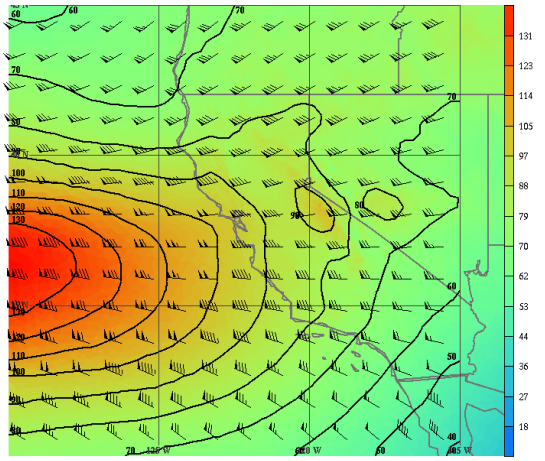

(a)

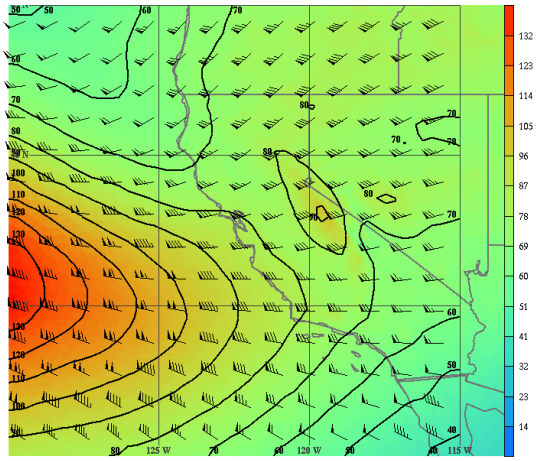

(b)

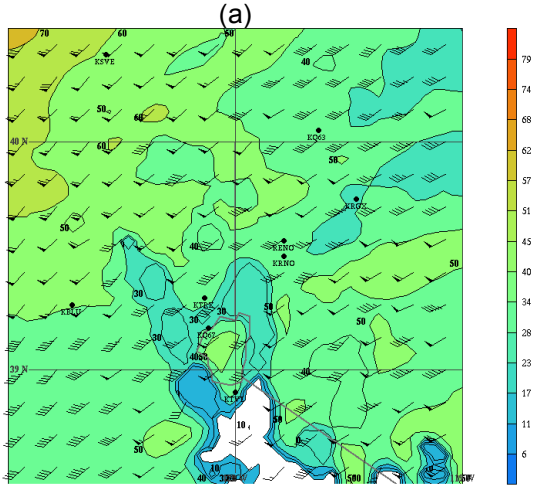

(c)

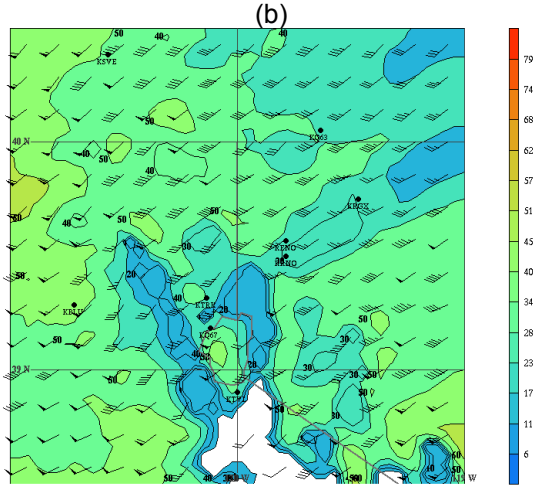

(d)

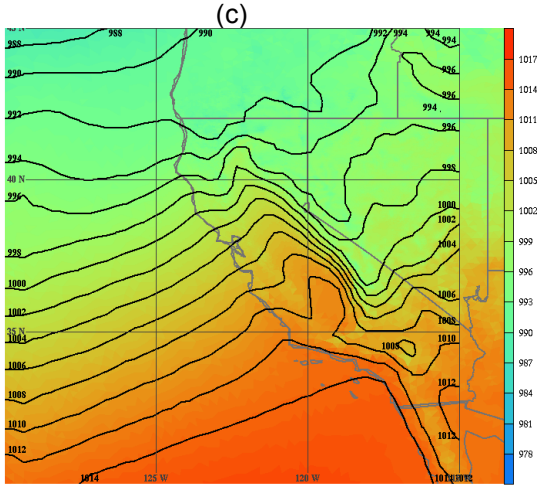

(e)

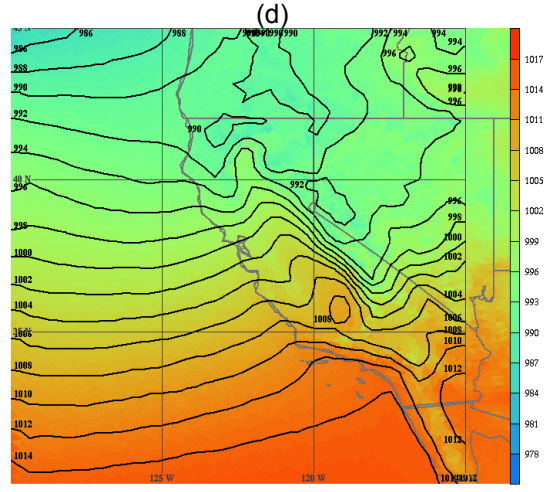

(f)

Figure 6: Figures 6a, 6b, 6e, and 6f are the same fields as Figures 5a, 5b, 5e, and 5f. 750 hPa isotachs and wind barbs for the (c) AVN and (d) NCEP/NCAR simulations. All times are for 1500 UTC 31 December 2005.

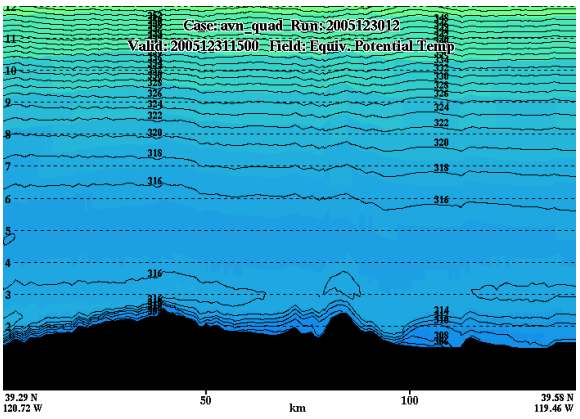

(g)

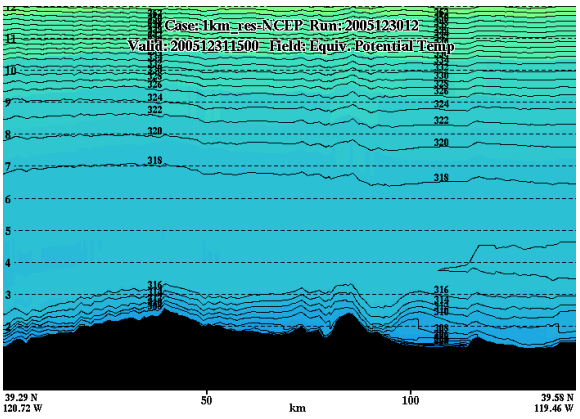

(h)

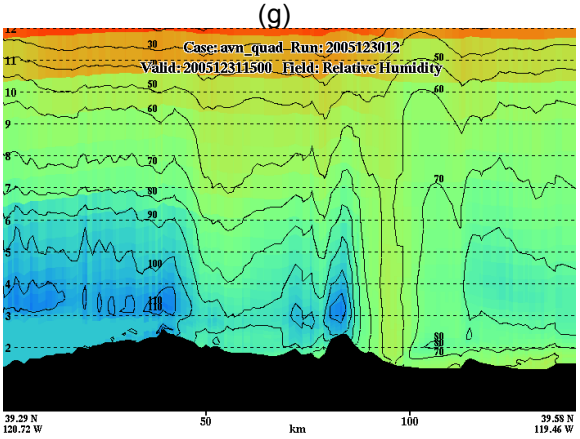

(i)

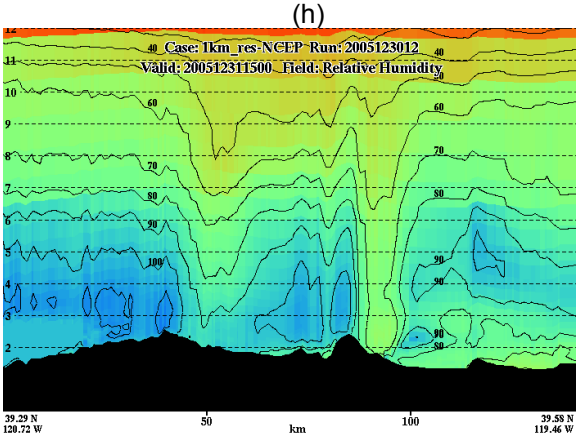

(j)

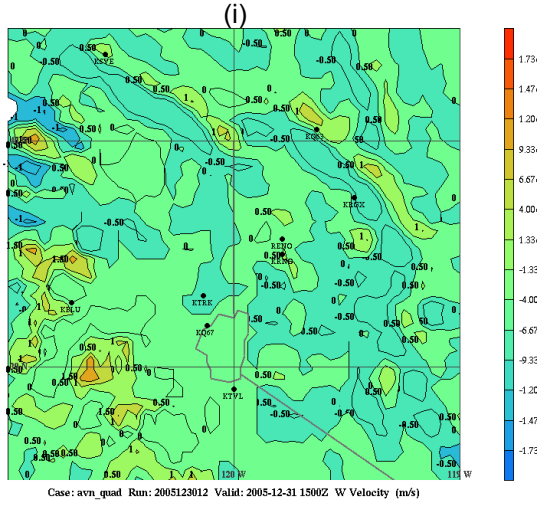

(k)

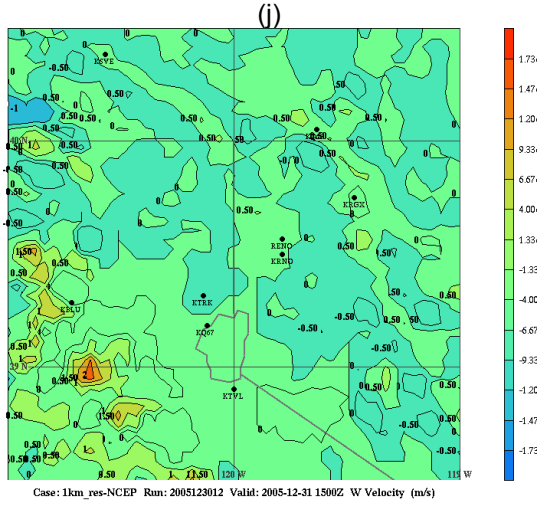

(l)

Figure 6 (cont.): Figures 6g-6l are the same fields as Figures 5g-5l except all times are for 1500 UTC 31 December 2005.

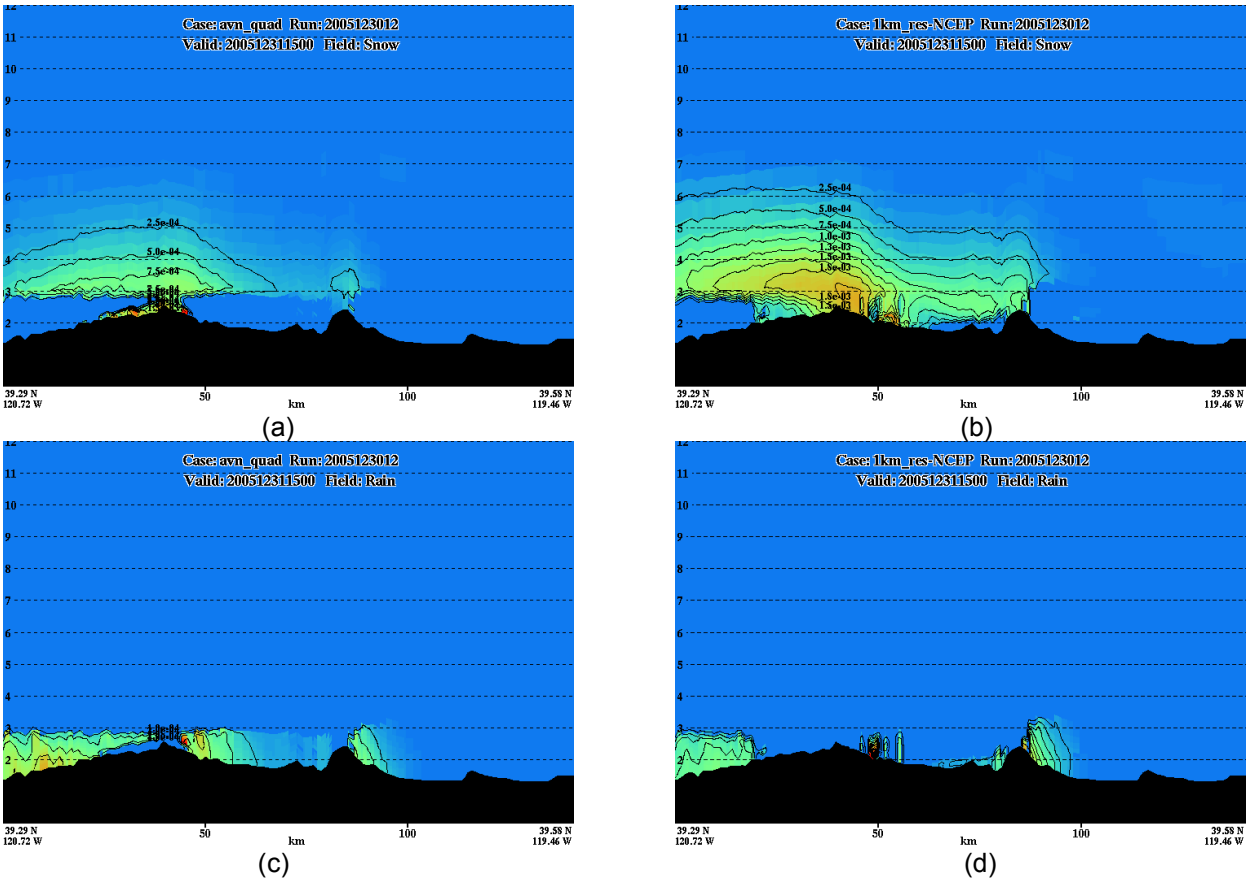

Figure 7: 1500 UTC December 31 2005 cross sections of (a and b) frozen and (c and d) liquid hydrometeors (kg m^{-3}) for the (a and c) AVN and (b and d) NCEP/NCAR reanalysis simulations. The contour intervals for the frozen and liquid hydrometeors are 2.5×10^{-4} and 1×10^{-4} kg m^{-3} respectively. The cross section coverage is the same as in Figures 5 and 6.

the NCEP/NCAR simulation is slightly potentially unstable while the AVN is not. The relative humidity cross sections for 0600 UTC 31 December (Figs. 5i and 5j) show there is an increase of relative humidity in the 3-5 km layer and less lee side drying in the NCEP/NCAR versus the AVN. The vertical motions in the simulations provide some very subtle differences. The intensities of the velocities are generally higher and more sinking motion is detected in the AVN simulation than the NCEP/NCAR simulation (Figs. 5k and 5l) due to increased low-level cross-mountain flow in the AVN simulation, but both do show an area of 50 cm s^{-1} moving from the Carson Range to the Reno-Carson City area at 800 hPa between 0000-0900 UTC 31 December. This would maintain low-level dynamic support for the first heavy precipitation event.

The second precipitation event has the jet streak at 250 hPa on 1500 UTC 31 December for the NCEP/NCAR data further to the south and more curved than the AVN data (Figs. 6a and 6b). This would suggest the ageostrophic winds have strong, along-flow directed ageostrophy in the exit region consistent with a balanced curved jet streak. The wind speed in the two simulations at 750 hPa on 1500 UTC 31 December (Figs. 6c and 6d) are similar to one another, but the direction given by the wind barbs show that there is more of a southerly component in the NCEP/NCAR simulation versus the AVN data, thus more curvature-induced divergence at low to mid levels. The MSLP for 1500 UTC 31 December (Figs. 6e and 6f) for both simulations show continuous deepening of the meso low on the lee side of the Carson Range. The MSLP for the AVN simulation is at 995 hPa and the NCEP/NCAR simulation is at 992 hPa at the same area. The θ_e cross section for 1500 UTC 31 December has a deep layer of vertically decreasing θ_e at mid levels for both simulations (Figs. 6g and 6h). The AVN data set produces a 3 km deep layer of 316 K and the

NCEP/NCAR reanalysis has a lapse rate of 2 K between 3 and 6.5 km, indicating more enhanced convective instability in the NCEP/NCAR relative to the AVN. The relative humidity cross sections for 1500 UTC 31 December (Figs. 6i and 6j) indicate that the overall depth of ≥ 90% relative humidity layer has increased as the NCEP/NCAR simulation continues to have a more moist profile than the AVN simulation. The vertical velocities at 800 hPa show even more subtle differences than the earlier times (Figs. 6k and 6l). The velocity trends remain the same compared to the earlier times, but there is a slight increase in the upward vertical velocity near Reno-Carson City area between 1200-1800 UTC 31 December 2005. At low to mid-levels, frozen hydrometeors were transported over the mountain crest, which subsequently melted into rain on to the lee side, thereby enabling the high amounts of spillover precipitation for this event on 1500 UTC 31 December 2005 (Figs. 7a-7d).

4. SUMMARY AND CONCLUSIONS

The cumulative precipitation totals for the two data sets display radical differences in amounts, thus indicating how much a difference in the initial state of the model can impact a forecast (Figs. 8a and 8b). At 0000 UTC 1 January 2006, the AVN data set produced rainfall totals of up to 8 inches on the windward side and up to the Sierra Crest and over 1.5 inches on the lee of the Carson Range (1 inch = 25.4 mm). Meanwhile, the NCEP/NCAR reanalysis data set produces over a foot of precipitation on the windward side and up to the Sierra Crest and nearly 6 inches on the lee of the Carson Range. The results show the NCEP/NCAR simulation produces a much higher rainfall total and more closely resembles the real world versus the AVN simulation. This is most pronounced in the spillover precipitation zone between Carson City and Reno.

Key differences in the two data sets lead to different simulation results. The first critical difference is there was more southerly momentum present in the NCEP/NCAR reanalysis data than in the AVN (ref. Figs. 6c and 6d). This low-level southerly momentum is consistent with more curvature in the upper-level polar jet exit regions. The second critical difference is more (predominantly) mid-level moisture in the NCEP/NCAR reanalysis initially versus the AVN (ref. Figs. 7a and 7b). When these two components force the downstream atmosphere, there is more moisture that is transported across the Sierra at an angle that is along the complex terrain instead of directly cross-mountain flow. In the cross-mountain flow regime, the relative humidity can be minimized due to downslope subsidence. *This means more moisture, instability and lift occur in the NCEP/NCAR simulation.* The most logical explanation that would lead to these

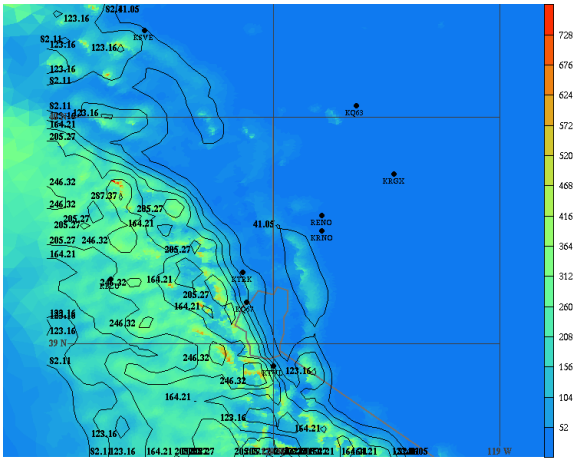

(a)

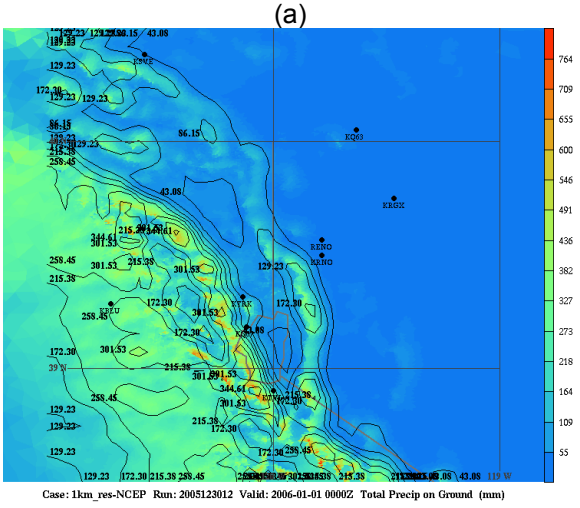

(b)

Figure 8: Cumulative rainfall amounts (mm) for 36 hour model simulation ending at 0000 UTC 1 January 2006 for the (a) AVN and (b) NCEP/NCAR reanalysis simulations.

differences in the two simulations is the amount of vertical levels and asynoptic data in both analyses' initial conditions. The AVN data did not have enough subsynoptic data structure, so important initial features were smoothed or missing.

Important features that required the spillover precipitation event to occur on the lee side of the Carson Range in to the Reno-Sparks-Carson City area for this event were the 1) jet exit region divergence of mass flux aloft, 2) the cold

front aloft producing 3) mid-level instability and moisture advection, 4) continual upward vertical motion, and 5) deepening the meso low as well as its accompanying 6) low-level return branch circulation for the duration of the event. The phasing of upper and lower-level jet streaks causes the low-level return branch circulation to experience ascent at low to mid levels. Together with mid-level moist air advection and cold air advection above can result in destabilization and moistening above and downstream from the mountain crest. These dynamics were all needed to produce heavy spillover precipitation.

Acknowledgments

We would like to thank the Science Applications International Corporation (SAIC) for use of the OMEGA model for our research purposes and Ken Waight of MESO Incorporated for providing the model data for our simulations. We would also like to thank the Reno National Weather Service Forecast Office for additional rain gauge data obtained from their meso network. This material is based upon work supported by the National Science Foundation under Grant No. 0447416 as well as UCAR/COMET Grant No. S06-58387, DOD/Army Grant No. N61339-04-C-0072, and a DRI/IPA Grant.

References

Anthes, R. A., 1977: A cumulus parameterization scheme utilizing a one-dimensional cloud model. *Mon. Wea. Rev.,* **105,** 270-286.

Bacon, D. P., N. N. Ahmad, Z. Boybeyi, T. J. Dunn, M. S. Hall, P. C. S. Lee, R. A. Sarma, M. D. Turner, K. T. Waight, S. H. Young, and J. W. Zack, 2000: A dynamically adapting weather and dispersion model: The operational multiscale environment model with grid adaptivity (OMEGA). *Mon. Wea. Rev.,* **128,** 2044-2076.

Browning, K. A., C. W. Parode, and F. F. Hill, 1975: The nature of orographic rain at wintertime cold fronts. *Quart. J. Roy. Meteor. Soc.,* **101,** 333-352.

Buzzi, A., N. Tartaglione, and P. Malguzzi, 1998: Numerical simulations of the 1994 Piedmont flood: Role of orography and moist processes. *Mon. Wea. Rev.,* **126,** 2369-2383.

Colle, B. A., 2004: Sensitivity of orographic precipitation to changing ambient conditions and terrain geometries: An idealized modeling perspective. *J. Atmos. Sci.,* **61,** 588-606.

Kalnay, E., and Co-Authors, 1996: The NCEP/NCAR 40-year reanalysis project. *Bull. Amer. Meteor. Soc.,* **77,** 437-471.

Kaplan, M. L., Y.-L. Lin, D. W. Hamilton, and R. A. Rozumalski, 1998: The numerical simulation of an unbalanced jetlet and its role in the Palm Sunday 1994 tornado outbreak in Alabama and Georgia. *Mon. Wea. Rev.,* **126,** 2133-2165.

Lin, Y.-H., R. D. Farley, and H. D. Orville, 1983: Bulk parameterization of the snow field in a cloud model. *J. Clim. Appl. Meteor.,* **22,** 1065-1092.

Locatelli, J. D., M. T. Stoelinga, R. K. Schwartz, and P. V. Hobbs, 1997: Surface convergence induced by cold fronts aloft and prefrontal surges. *Mon. Wea. Rev.,* **125,** 2808-2820.

Maddox, R. A., L. R. Hozit, C. F. Chappel, and F. Caracena, 1978: Comparison of meteorological aspects of Big Thompson and Rapid City flash floods. *Mon. Wea. Rev.,* **106,** 375-389.

Sinclair, M. R., 1994: A diagnostic model for estimating orographic precipitation. *J. Appl. Meteor.,* **33,** 1163-1175.

-------, D. S. Wratt, R. D. Henderson, and W. R. Gray, 1997: Factors affecting the distribution and spillover of precipitation in the Southern Alps of New Zealand--A case study. *J. Appl. Meteor.,* **36,** 428-442.

Uccellini, L. W., and D. R. Johnson, 1979: The coupling of upper and lower-troposphere jet streaks and implications for the development of severe convective storms. *Mon. Wea. Rev.,* **107,** 662-673.